Exchange-dominated spin waves in simple cubic antiferromagnetic films

J. Milton Pereira, Jr. and M. G. Cottam
Department of Physics and Astronomy, University of Western Ontario, London, Ontario, Canada N6A 3K7
(Received 28 June 2000; published 11 April 2001)

A study is made of the role of surface orientation in determining the spectra of surface spin waves in antiferromagnetic films. The calculations apply to the exchange-dominated regime and are based on a spin-wave operator and Green-function technique. The method exploits some properties of banded (tridiagonal and pentadiagonal) matrices in order to find analytical expressions for the spin-wave frequencies. Theoretical results are presented for films with a simple cubic structure and surfaces corresponding to three different orientations of the crystal planes, namely, (001), (011), and (111), for which the surface spin-wave characteristics are found to be quite distinct. This work generalizes previous calculations for semi-infinite simple cubic antiferromagnets with (001) surfaces.

DOI: 10.1103/PhysRevB.63.174431 PACS number(s): 75.30.Ds, 75.70.−i

I. INTRODUCTION

It is known that the spin dynamics of a large class of ordered magnetic materials can be well described by models that include the short-range exchange coupling between magnetic sites but disregard the long-range magnetic dipole-dipole interactions. This is often the case for antiferromagnets in appropriate wave-vector regimes and results from the greater strength of the exchange coupling as compared to the other interactions in the system (see, e.g., Ref. 1). The dipolar interactions eventually become important for the spin-wave dispersion at very small wave vector. In the exchange-dominated regime the dynamics of the low-lying spin excitations depends sensitively on the crystal structure, since that determines the positions of nearest neighbors for each magnetic site.

For thin films another factor that influences the properties of the magnetic excitations is the orientation of the crystal planes at the surfaces. This determines the number of missing bonds per site at the surfaces and also modifies the symmetry of the interactions between the layers in different directions on the surfaces.[2,3] As a consequence, the spectra of the magnetic modes in a film might display distinct features that depend on the orientation of the growth direction. This should be particularly the case in antiferromagnets where there are two sublattices of spin sites.

Usually, in order to obtain the spin wave (SW) spectrum from a microscopic approach, one constructs the linearized equations of motion for either the spin operators at each crystal site or, alternatively, for the spin-dependent Green functions.[4] Often the spin operators are transformed to a representation in terms of boson creation and anihilation operators. The resulting system of coupled equations can then be written as a matrix equation. In these formalisms the calculation of the frequencies of the surface SW modes on a film with N atomic layers depends on the inversion of a $N\times N$ (or larger) matrix which cannot, save in some particular cases, be carried out analytically.

In this paper we describe an analytical procedure for calculating the frequencies of SW modes in simple cubic antiferromagnetic thin films in the exchange-dominated regime. We use the fact that, due to the short range of the coupling between the magnetic sites, the equations of motion can be written in a form that involves banded matrices (e.g., tridiagonal, pentadiagonal, etc.) The method consists of rewriting the equations of motion in such a way that the corresponding matrix equation can be recast into a form with a known analytical solution. The approach is different from, and simpler than, that used by Wolfram and Dewames for a semi-infinite simple-cubic antiferromagnet with a (001) surface.[2] By contrast, it enables us to obtain calculations for finite-thickness films and for other surface orientations.

We present results showing the effect of finite film thickness in coupling the SW modes localized near the two surfaces, leading to a splitting of several of the surface SW mode branches that occur in the semi-infinite limit. Also in a film the bulk SW modes become quantized. The results are obtained for films with surfaces corresponding to three different crystallographic planes, namely, (001), (011), and (111). It is discussed here how each orientation modifies the coupling scheme between the sites in each layer and the equivalence of the sublattices, as well as introducing directional effects in the dispersion relations of the SW modes.

In order to introduce the basic method, let us first review the case of a ferromagnet in the exchange-dominated regime. The Heisenberg Hamiltonian has the form

$$\mathcal{H}=-\frac{1}{2}\sum_{i,j} J_{ij}\mathbf{S}_i\cdot\mathbf{S}_j-g\mu_B H_0\sum_i S_i^z+\mathcal{H}_{\text{anis}}, \qquad (1)$$

where J_{ij} is the exchange coupling between sites i and j, and H_0 is an applied magnetic field in the z direction (the direction of spin ordering). The term $\mathcal{H}_{\text{anis}}$ represents uniaxial single-ion anisotropy, which may be different at a surface. We consider a film geometry with the magnetic sites occupying layers in the xy plane that are labeled by the index n (where $n=1,2,\ldots,N$ for a film with N layers). The SW dispersion relations can be studied by writing down the operator equation of motion for S_i^+ obtained using $\mathcal{H}$ and the random phase approximation at $T\ll T_c$ while assuming $\langle S_i^z\rangle = S$ for the ferromagnet. Taking a time dependence such as $\exp(i\omega t)$ where ω is the mode frequency, we have

$$\left[\omega - g\mu_B(H_0+H_{Ai}) - S\sum_j J_{ij}\right]S_i^+ + S\sum_j J_{ij}S_j^+ = 0, \tag{2}$$

where H_{Ai} denotes the effective anisotropy field at site i. Next, using the translational symmetry parallel to the layers, we write $S_i^+ = s_n(\mathbf{k})\exp(-i\mathbf{k}\cdot\mathbf{r}_i^{\parallel})$ where $\mathbf{k}=(k_x,k_y)$ is a two-dimensional (2D) in-plane wave vector and $\mathbf{r}_i^{\parallel}=(x_i,y_i)$. Equation (2) may then be expressed in matrix form as

$$(\mathbf{A}-\mathbf{R})\mathbf{s}=0, \tag{3}$$

where $\mathbf{s}$ is the column matrix with s_n in the nth row, $\mathbf{A}$ is a $N\times N$ matrix involving only the bulk parameters of the film, and $\mathbf{R}$ describes the perturbing effects due to the surfaces (i.e., due to missing exchange bonds, as well as due to modified values of the surface exchange and anisotropy parameters). Denoting $\mathbf{B}\equiv\mathbf{A}^{-1}$ and rearranging Eq. (3), it can be shown[4] that the surface SW modes of the film can be obtained from the condition

$$\det(\mathbf{I}-\mathbf{BR})=0. \tag{4}$$

For example, in the application to a simple-cubic (sc) ferromagnetic film with (001) surfaces and nearest-neighbor exchange coupling only, $\mathbf{A}$ is a tridiagonal matrix,[4] i.e., its nonzero elements can be written as $[\mathbf{A}]_{l,m}=D\delta_{l,m}-\delta_{l-1,m}-\delta_{l+1,m}$, where $D=6-2[\cos(k_xa)+\cos(k_ya)]-[\omega-g\mu_B(H_0+H_A)]/SJ$, with a and H_A denoting the lattice parameter and the bulk anisotropy field, respectively. The elements of the inverse of $\mathbf{A}$ are given explicitly by[4]

$$[\mathbf{A}^{-1}]_{l,m}=\frac{x^{l+m}-x^{|l-m|}+x^{2N+2-l-m}-x^{2N+2-|l-m|}}{(1-x^{2N+2})(x-x^{-1})}, \tag{5}$$

where the complex parameter x is defined by $x+x^{-1}=D$ and $|x|\leqslant 1$. The matrix $\mathbf{R}$, on the other hand, has elements equal to zero everywhere except in two small blocks of dimension $n_0\times n_0$ located at the ends of the leading diagonal. Typically, for a sc (001) ferromagnetic film, n_0 may be 1, 2, or 3, depending on the missing bonds and on assumptions regarding the modified exchange and anisotropy parameters near the surfaces.[4] The solution of Eq. (4) then reduces to solving a $2n_0\times 2n_0$ determinantal condition.

This tridiagonal matrix method, either in conjunction with the operator equation of motion or the Green function equation of motion, has been applied to a range of problems involving exchange surface SW (e.g., see Refs. 4–7, and references therein). In the following examples we generalize the procedure to sc antiferromagnetic thin films, where the presence of two sublattices generates equations with more complicated banded matrices.

II. SIMPLE CUBIC ANTIFERROMAGNETIC FILMS WITH (001) SURFACES

Let us consider a two-sublattice antiferromagnetic thin film with N atomic layers (in the xy plane), sc structure and (001) surfaces (see Fig. 1). The Hamiltonian is written as

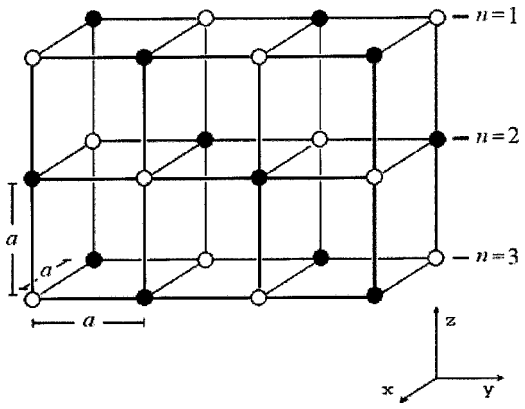

FIG. 1. Schematic view of an antiferromagnetic film with sc structure and surfaces corresponding to the (001) crystallographic planes.

$$\mathcal{H}=\sum_{i,j} J_{ij}\mathbf{S}_i\cdot\mathbf{S}_j - g\mu_B\sum_i (H_0+H_{Ai})S_i^z - g\mu_B\sum_j (H_0-H_{Aj})S_j^z, \tag{6}$$

where J_{ij} is now the nearest-neighbor exchange between sites i and j on opposite sublattices (labeled u and d for spin ''up'' and spin ''down,'' respectively), and H_{Ai} and H_{Aj} are effective anisotropy fields. The magnitudes of the anisotropy field (equal and opposite on the two sublattices) are taken to have the bulk value H_A everywhere, except in the surface layers where it may take the values H_{AS} and H'_{AS} for $n=1$ and N, respectively. Likewise J_{ij} has the bulk value J, except when both spins are in the same surface layer and it has the values J_S and J'_S. Calculations for the surface SW in *semi-infinite* sc antiferromagnets were made by Wolfram and Dewames.[2] By contrast the matrix technique, as later employed here, is more straightforward, allowing us to extend the studies to thin films where the presence of two surfaces provides coupling effects between the modes.

As before, the equations of motion for the S^+ operators are transformed to a representation using the 2D wave vector $\mathbf{k}$ and layer index n. Additionally, the operators now have a sublattice label (u or d). In this surface orientation, each layer contains both u and d sublattice spins. The spin amplitudes are then transformed to symmetric and antisymmetric combinations by defining $s_n\equiv s_n^{(u)}+s_n^{(d)}$ and $\overline{s_n}\equiv s_n^{(u)}-s_n^{(d)}$. The equations of motion become

$$\begin{aligned}
E\overline{s}_1 &= [1+\epsilon(4-\gamma_{\mathbf{k}})+\omega_S]\overline{s}_1-\overline{s}_2,\\
E\overline{s}_n &= (6+\omega_A-\gamma_{\mathbf{k}})\overline{s}_n-\overline{s}_{n-1}-\overline{s}_{n+1},\quad 1<n<N,\\
E\overline{s}_N &= [1+\epsilon'(4-\gamma_{\mathbf{k}})+\omega'_S]\overline{s}_N-\overline{s}_{N-1},
\end{aligned} \tag{7}$$

$$\begin{aligned}
E\overline{s}_1 &= [1+\epsilon(4-\gamma_{\mathbf{k}})+\omega_S]s_1+s_2\\
E\overline{s}_n &= (6+\omega_A-\gamma_{\mathbf{k}})s_n+s_{n-1}+s_{n+1},\quad 1<n<N,\\
E\overline{s}_N &= [1+\epsilon'(4-\gamma_{\mathbf{k}})+\omega'_S]s_N+s_{N-1},
\end{aligned} \tag{8}$$

where we have defined $\gamma_{\mathbf{k}}=2[\cos(k_x a)+\cos(k_y a)]$ as a structure factor, $\omega_A=g\mu_B H_A/SJ$, and $E=(\omega-g\mu_B H_0)/SJ$. The surface parameters are $\omega_S=g\mu_B H_{AS}/SJ$, $\omega_S'=g\mu_B H_{AS}'/SJ$, $\epsilon=J_S/J$, and $\epsilon'=J_S'/J$. The s terms can now be eliminated from these two sets of coupled equations. The result (for the s_n) may be expressed in the same form as Eq. (3), except that **A** becomes a pentadiagonal matrix, i.e., its nonzero elements occur in a band of five diagonals centered around the leading diagonal. However, we find that this pentadiagonal matrix is expressible as the product of two tridiagonal matrices $\mathbf{A}_1$ and $\mathbf{A}_2$, plus a difference term that is absorbed in the definition of **R**. The two tridiagonal matrices have elements defined by

$$[\mathbf{A}_{1,2}]_{l,m}=D_{1,2}\delta_{l,m}-(\delta_{l-1,m}+\delta_{l+1,m}), \tag{9}$$

with $D_{1,2}(k_x,k_y,\omega)=-\gamma_{\mathbf{k}}\pm\omega_0$, where $\omega_0\equiv\sqrt{(\omega_A+6)^2-E^2}$. These matrices obey the relation $\mathbf{A}_1-\mathbf{A}_2=(D_1-D_2)\mathbf{I}$ and as a consequence, the inverse of their product satisfies

$$(\mathbf{A}_1\mathbf{A}_2)^{-1}=\frac{1}{(D_1-D_2)}(\mathbf{A}_2^{-1}-\mathbf{A}_1^{-1}). \tag{10}$$

Thus, using Eq. (5) for the inverse of a tridiagonal matrix, the elements of $\mathbf{B}\equiv(\mathbf{A}_1\mathbf{A}_2)^{-1}$ are

$$[\mathbf{B}]_{l,m}=(2\omega_0)^{-1}\left[\frac{y^{l+m}-y^{|l-m|}+y^{2N+2-l-m}-y^{2N+2-|l-m|}}{(1-y^{2N+2})(y-y^{-1})}-\frac{x^{l+m}-x^{|l-m|}+x^{2N+2-l-m}-x^{2N+2-|l-m|}}{(1-x^{2N+2})(x-x^{-1})}\right], \tag{11}$$

where $x+x^{-1}=D_1$ and $y+y^{-1}=D_2$ (with $|x|\leqslant 1$ and $|y|\leqslant 1$).

The matrix **R** has only a few nonzero elements, which are listed in the Appendix. The implicit SW dispersion relation becomes $\det\mathbf{C}=0$, where **C** is a 4×4 matrix with elements defined in the Appendix. The dispersion relation of the surface SW modes are now found as the solutions corresponding to $|x|<1$ and $|y|<1$ (a localization condition). There is some simplification of the analytical result in the case of films with symmetric surfaces ($\sigma=\sigma'$ and $\epsilon=\epsilon'$), when the determinantal condition yields

$$R_{1,1}(B_{1,1}\pm B_{1,N})+(R_{1,2}+R_{2,1})(B_{1,2}\pm B_{2,N})-R_{1,2}R_{2,1}[(B_{1,2}\pm B_{2,N})^2-(B_{1,1}\pm B_{1,N})(B_{2,2}\pm B_{2,N-1})]-1=0. \tag{12}$$

The upper and lower sets of signs in Eq. (12) refer to modes that are symmetric and antisymmetric, respectively, with respect to the midpoint of the film. Also, we note that in the limit of $N\to\infty$ the elements $B_{1,N}$, $B_{2,N-1}$, and $B_{2,N}$ vanish, and the surface SW dispersion relation can be expressed as

$$R_{1,1}(y-x)+(R_{1,2}+R_{2,1})(y^2-x^2)+R_{1,2}R_{2,1}(\omega_0)^{-1}\times(y-x)^2(1-xy)-\omega_0=0. \tag{13}$$

By contrast, the frequencies of the quantized bulk modes of the film are found as the solutions of $\det\mathbf{C}=0$ with $|x|=|y|=1$. The SW modes in this case are all doubly degenerate when $H_0=0$. For the (001) case the resulting dispersion relation is expressible in the form

$$E^2=(\omega_A+6)^2-4[\cos(k_x a)+\cos(k_y a)+\cos(\alpha a)]^2, \tag{14}$$

where α takes a set of real discrete values ($0\leqslant\alpha\leqslant\pi/a$) that can be deduced from the determinantal condition. As $N\to\infty$ the bulk modes become closer together, forming an effective continuum.

Numerical results are shown in Figs. 2 and 3, where the values of ω/SJ for the surface SW branches are plotted

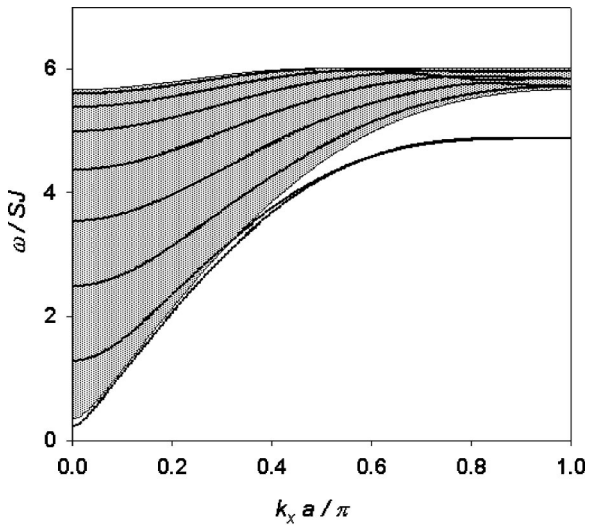

FIG. 2. SW dispersion relations for sc antiferromagnetic films with (001) surfaces, taking $\omega_A=10^{-2}$, $\sigma=1$, $\epsilon=1$, and $N=8$. The bulk modes are those within the shaded region.

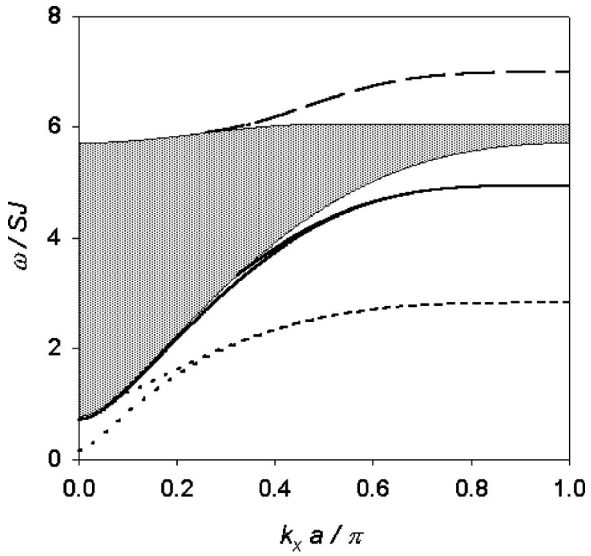

FIG. 3. Comparison of surface SW dispersion relations for sc antiferromagnetic films with (001) surfaces, taking $\omega_A=5\times10^{-2}$ and $\sigma=1$. The sets of curves correspond to $\epsilon=1$ (solid), $\epsilon=0.5$ (dotted), and $\epsilon=1.5$ (dashed). The region containing the bulk modes is shaded.

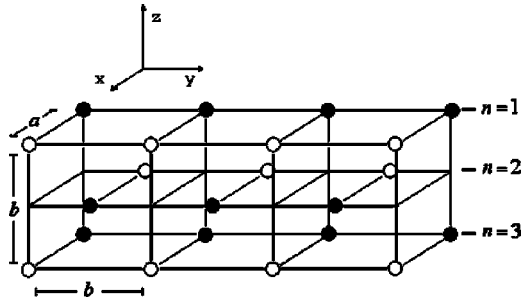

FIG. 4. Representation of an antiferromagnetic film with sc structure and surfaces corresponding to the (011) crystallographic planes. The distance between each layer is $b/2$, where $b \equiv a\sqrt{2}$. The neighboring sites in the same layer are directly coupled by the nearest-neighbor exchange only along the x axis.

against $k_x a/\pi$, taking $\mathbf{k}=(k_x,0)$. In fact Fig. 2 shows both the quantized SW bulk modes (inside the shaded area) and the surface SW modes (outside the shaded area) for a film with 8 layers, taking $\omega_A=10^{-2}$, $\sigma=1$ and $\epsilon=1$. The surface SW modes are seen to split into two branches for small wave vectors, as expected from Eq. (19), and they become approximately degenerate at larger k_x. Figure 3 displays the surface SW modes for three different values of ϵ, again for symmetric film surfaces, taking $\omega_A=5\times10^{-2}$ and with other parameters as before. Again the shaded area corresponds to the region occupied by the bulk modes, but the individual modes are not shown since these would be different for each value of ϵ. For $\epsilon=0.5$ and 1, the branches correspond to acoustic surface modes and are situated below the bulk region. For $\epsilon=1.5$ we obtain two degenerate optical surface modes (above the bulk region) that are truncated. For sufficiently small values of ϵ (when $\sigma=1$), the assumed antiferromagnetic ground state can become unstable, corresponding to a reorientation of spins near the surfaces. This is analogous to the type of surface reorientation phase transition discussed by Mills[8] in certain anisotropic ferromagnets. In our case it only occurs when the surface perturbations (in exchange or anisotropy) are large, and it can in principle occur for other surface orientations.

III. SIMPLE CUBIC ANTIFERROMAGNETIC FILMS WITH (011) SURFACES

We next consider a sc antiferromagnetic film with (011) surfaces, described by the same Hamiltonian as in Eq. (6). What distinguishes the formalism for this orientation from the previous one is that the spins in each layer now form a rectangular 2D net with sides of length a (along the x axis), and $\sqrt{2}a$ (along y). More important, the terms describing the interactions of nearest neighbors in adjacent layers are different in the x and y directions (see Fig. 4). As a result, there are distinct properties expected for the SW modes propagating along each direction. The formalism for obtaining the SW frequencies is, however, similar to the previous case. Each layer in the film contains equal numbers of sites from both sublattices and the spin amplitudes are transformed to obtain the equations of motion

$$
\begin{aligned}
Es_1 &= [2+2\epsilon+\omega_S-\epsilon\gamma_{\mathbf{k}}^{(x)}]\bar{s_1}-\gamma_{\mathbf{k}}^{(y)}\bar{s_2},\\
Es_n &= [6+\omega_A-\gamma_{\mathbf{k}}^{(x)}]\bar{s_n}-\gamma_{\mathbf{k}}^{(y)}(\bar{s}_{n-1}+\bar{s}_{n+1}),\ 1<n<N,\\
Es_N &= [2+2\epsilon'+\omega_S'-\epsilon'\gamma_{\mathbf{k}}^{(x)}]\bar{s_N}-\gamma_{\mathbf{k}}^{(y)}\bar{s}_{N-1}, \qquad (15)\\
E\bar{s_1} &= [2+2\epsilon+\omega_S+\epsilon\gamma_{\mathbf{k}}^{(x)}]s_1+\gamma_{\mathbf{k}}^{(y)}s_{n+1},\\
E\bar{s_n} &= [6+\omega_A+\gamma_{\mathbf{k}}^{(x)}]s_n+\gamma_{\mathbf{k}}^{(y)}(s_{n-1}+s_{n+1}),\ \ 1<n<N,\\
E\bar{s_N} &= [2+2\epsilon'+\omega_S'+\epsilon'\gamma_{\mathbf{k}}^{(x)}]s_N+\gamma_{\mathbf{k}}^{(y)}s_{N-1} \qquad (16)
\end{aligned}
$$

with $\gamma_{\mathbf{k}}^{(x)}=2\cos(k_x a)$, $\gamma_{\mathbf{k}}^{(y)}=2\cos(k_y a/\sqrt{2})$, and other definitions as Sec. II. The $\bar{s_n}$ amplitudes are then eliminated as before and another product of two tridiagonal matrices is obtained by decomposing a pentadiagonal matrix. The tridiagonal matrices are defined as

$$
[\mathbf{A}_{1,2}]_{l,m}=D_{1,2}\delta_{l,m}-\gamma_{\mathbf{k}}^{(y)}(\delta_{l-1,m}+\delta_{l+1,m}), \qquad (17)
$$

with $D_{1,2}=-\gamma_{\mathbf{k}}^{(x)}\pm\omega_0$.

The dispersion relation is again obtained from a 4×4 determinantal condition which is formally the same as in Sec. II, but with the above redefinitions. From the expressions for the matrix elements, it can be seen that the direction of propagation of the SW modes along the surface plays an important role in this case, since the k_x and k_y components of the wave vector are present in different diagonals. The bulk modes are the solutions with $|x|=1$ and $|y|=1$, which leads to a dispersion relation of the form

$$
\begin{aligned}
E^2=(\omega_A+6)^2-[&2\cos(k_x a)\\
&+4\cos(k_y a\sqrt{2})\cos(\alpha a\sqrt{2}/2)]^2, \qquad (18)
\end{aligned}
$$

where α takes discrete values.

Numerical results are shown for the surface SW modes in Figs. 5 and 6, where the values of ω/SJ are obtained for the propagation wave vector $\mathbf{k}$ along the x and y axes, respectively. In these examples we have taken a symmetric film with $N=8$, $\omega_A=10^{-2}$ and $\sigma=1$. Figure 5 displays the results for propagation along the x direction for two values of ϵ. For $\epsilon=1.0$ there are two acoustic surface SW modes (dashed lines) that become degenerate for larger wave vectors, while for $\epsilon=2.5$ we find two optical, truncated, surface SW branches (solid lines). The shaded region corresponds to the region of quantized bulk modes. Figure 6 shows the surface SW branches for modes propagating along the y direction for surfaces with $\epsilon=1.0$ and 1.5. For $\epsilon=1.0$ (dashed lines) the branches show a similar behavior to those in Fig. 5. However, in contrast with the previous figure, there are no optical modes until $\epsilon>4$ (for $\sigma=1$).

IV. SIMPLE CUBIC ANTIFERROMAGNETIC FILMS WITH (111) SURFACES

In the (111) orientation, each layer of the film contains sites of only one sublattice type, with the ''up'' and ''down'' layers alternating, while the spins in each layer form a triangular 2D net with sides of length $a\sqrt{2}$ (see Fig. 7). As a

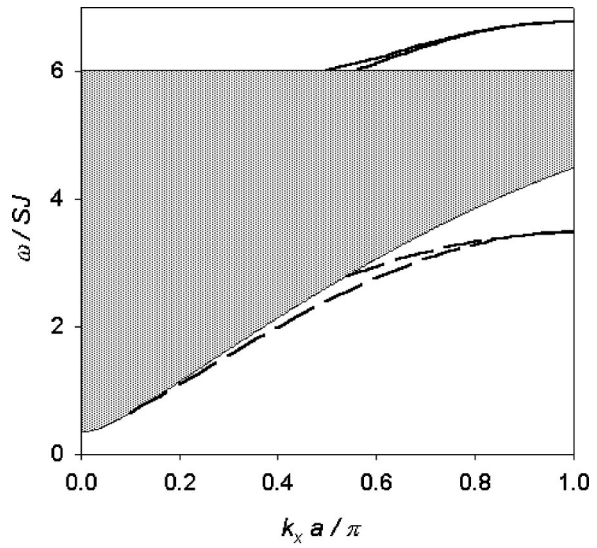

FIG. 5. Surface SW dispersion relations for sc antiferromagnetic films with (011) surfaces, for propagation along the x axis, taking $N=8$, $\omega_A=10^{-2}$, and $\sigma=1$. The curves correspond to $\epsilon=1.0$ (dashed) and $\epsilon=2.5$ (solid). The region containing the bulk modes is shaded.

consequence, the characteristics of the SW modes depend not only on the number of layers N but also on whether this number is even or odd. In the latter case both surfaces are of the same sublattice type (e.g., both u), whereas in the former case the two surface layers are of different sublattice types (one u, one d). In order to make explicit this difference in the equations of motion, the layers for each sublattice are individually labeled as in Fig. 7.

Let us consider initially the case of a film with an even

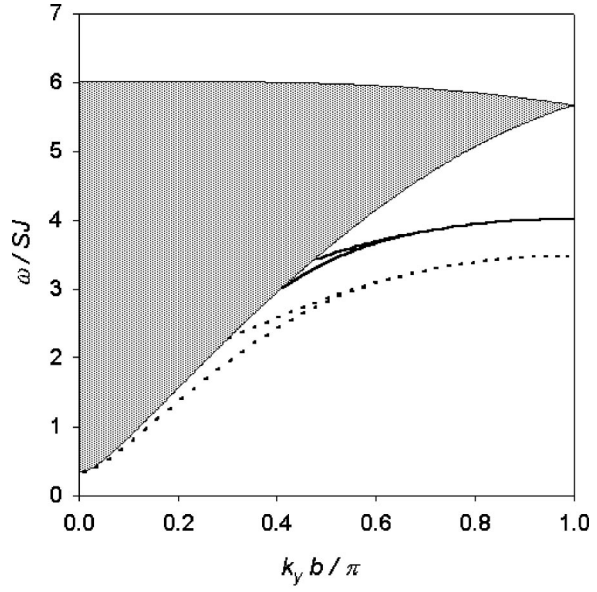

FIG. 6. Surface SW dispersion relations for sc antiferromagnetic films with (011) surfaces, for propagation along the y axis, taking $N=8$, $\omega_A=10^{-2}$, and $\sigma=1$. The curves correspond to $\epsilon=1.0$ (dotted) and $\epsilon=1.5$ (solid). The region containing the bulk modes is shaded.

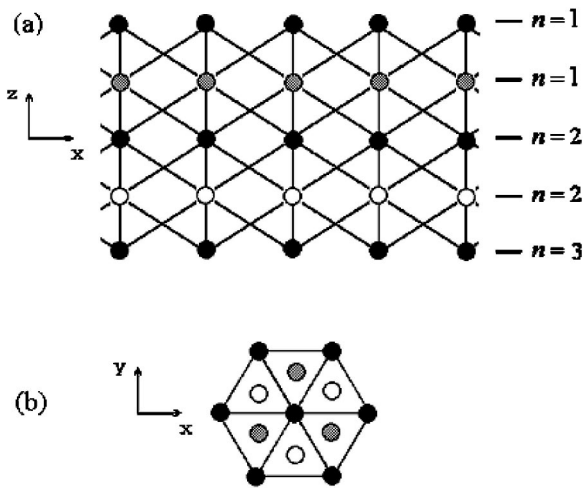

FIG. 7. Schematic representation of an antiferromagnetic film with sc structure and surfaces corresponding to the (111) crystallographic planes, viewed (a) parallel and (b) perpendicular to the surface planes. The magnetic sites in each layer are arranged in a triangular lattice. The black dots correspond to sites of sublattice u, and the white and shaded dots are sites of sublattice d. The layer numbering is shown.

number of layers, denoting $N=2M$ where M is an integer. Thus, using assumptions about the surface perturbations in the exchange and anisotropy field as before, the linearized equations of motion for the spin amplitudes become, in matrix form

$$\mathbf{A}_1\mathbf{s}^{(u)}=[\mathbf{\Xi}_\mathbf{k}-\mathbf{\Delta}_\mathbf{k}]\mathbf{s}^{(d)}, \quad \mathbf{A}_2\mathbf{s}^{(d)}=-[\mathbf{\Xi}^\dagger{}_\mathbf{k}-\mathbf{\Delta}^*{}_\mathbf{k}]\mathbf{s}^{(u)}, \tag{19}$$

where the elements of the $M\times M$ matrices are defined as

$$[\mathbf{A}_1]_{m,n}=\omega_1\delta_{m,n}+g\,\delta_{1,n}+h'\,\delta_{M,n}, \tag{20}$$

$$[\mathbf{A}_2]_{m,n}=\omega_2\delta_{m,n}-g'\,\delta_{M,n}-h\,\delta_{1,n}, \tag{21}$$

$$[\mathbf{\Xi}_\mathbf{k}]_{m,n}=\xi_\mathbf{k}\delta_{m,n}+\xi_\mathbf{k}{}^*\,\delta_{m-1,n}, \tag{22}$$

$$[\mathbf{\Delta}_\mathbf{k}]_{m,n}=\xi_\mathbf{k}[(1-\epsilon)\,\delta_{1,n}+(1-\epsilon')\,\delta_{M,n}]. \tag{23}$$

Due to the triangular geometry within each layer, the dynamic aspect of the exchange interaction is now described by a *complex* structure factor

$$\xi_\mathbf{k}=\exp\left(ik_y a\sqrt{\frac{6}{3}}\right)+2\cos\left(k_x a\sqrt{\frac{2}{2}}\right)\exp\left(-ik_y a\sqrt{\frac{6}{6}}\right), \tag{24}$$

and the other terms are $\omega_1=E-(6+\omega_A)$, $\omega_2=E+(6+\omega_A)$, $g=[6-3\epsilon+(1-\sigma)\omega_A]$, $h=3(1-\epsilon)$, $g'=[6-3\epsilon'+(1-\sigma')\omega_A]$, and $h'=3(1-\epsilon')$. From Eq. (19) we can now obtain two matrix equations similar to Eq. (3) one for $\mathbf{s}^{(u)}$ and one for $\mathbf{s}^{(d)}$, that yield the SW frequencies. The equations can be written in the form

$$[\mathbf{A}-\mathbf{R}^{(\alpha)}]\mathbf{s}^{(\alpha)}=0, \tag{25}$$

where α denotes u or d, $\mathbf{A}$ is an *asymmetric* tridiagonal matrix

$$[\mathbf{A}]_{m,n}=D\delta_{m,n}-(\xi_{\mathbf{k}})^2\delta_{m-1,n}-(\xi_{\mathbf{k}}{}^*)^2\delta_{m+1,n}, \quad (26)$$

and the diagonal elements are given by $D=-2\xi_{\mathbf{k}}\xi_{\mathbf{k}}{}^*+\omega_0^2$. Note that $\mathbf{A}$ depends only on the bulk parameters, while all the surface effects are contained in $\mathbf{R}^{(u)}$ and $\mathbf{R}^{(d)}$, which are defined in the Appendix. By analogy with the previous cases, the dispersion relation of the SW modes can be deduced from the determinantal conditions $\det(\mathbf{I}-\mathbf{R}^{(u)}\mathbf{B})=0$ or $\det(\mathbf{I}-\mathbf{R}^{(d)}\mathbf{B})=0$, with $\mathbf{B}\equiv\mathbf{A}^{-1}$. Generalizing Eq. (5), the elements of the $\mathbf{B}$ matrix are

$$[\mathbf{B}]_{l,m}=\frac{\beta^{2l}x^{l+m}-x^{m-l}+\beta^{N+2-2m}x^{N+2-l-m}-\beta^{N+2-2m+2l}x^{N+2-(m-l)}}{\xi_{\mathbf{k}}{}^2[1-\beta^{N+2}x^{N+2}][\beta^2x-x^{-1}]}, \quad l\leqslant m, \quad (27)$$

$$[\mathbf{B}]_{l,m}=\frac{\beta^{2l}x^{l+m}-\beta^{2(l-m)}x^{l-m}+\beta^{N+2-2m}x^{N+2-l-m}-\beta^{N+2}x^{N+2-(l-m)}}{\xi_{\mathbf{k}}{}^2[1-\beta^{N+2}x^{N+2}][\beta^2x-x^{-1}]}, \quad l>m, \quad (28)$$

where $\beta\equiv\xi_{\mathbf{k}}{}^*/\xi_{\mathbf{k}}$ and $(\xi_{\mathbf{k}})^2x+(\xi_{\mathbf{k}}{}^*)^2x^{-1}=D$. The determination of the SW modes then reduces to solving $\det\mathbf{C}^{(u)}=0$ or $\det\mathbf{C}^{(d)}=0$, where $\mathbf{C}^{(u)}$ and $\mathbf{C}^{(d)}$ are 3×3 matrices in the present case (see the Appendix).

When N is odd (denoting $N=2M+1$) the influence of the Nth layer can be treated as an effective energy-dependent surface perturbation applied to the previous case for an even number of layers. This comes about by means of the identity

$$s^{(u)}{}_{M+1}=\frac{\epsilon'\xi_{\mathbf{k}}{}^*}{E-(3\epsilon'+\omega_S')}s^{(d)}{}_M, \quad (29)$$

which follows from the original equations of motion.

The two determinantal conditions are found to give the same result, due to degeneracy of the SW modes in this case. Some numerical results are shown in Figs. 8 and 9 for the values of ω/SJ of surface SW modes in films with symmetric surfaces ($\epsilon=\epsilon',\sigma=\sigma'$) having 8 and 9 layers, respectively. The propagation is chosen to be along the x direction with $\omega_A=10^{-2}$ and $\sigma=1$. The shaded area corresponds to the region of quantized bulk modes. In Fig. 8, for a film with $N=8$, there is just one acoustic surface SW branch for $\epsilon=1$ (solid line). However, if the value of ϵ is decreased there are two acoustic surface SW branches, with the higher frequency ones emerging from the bulk region for large wave vectors, as can be seen for $\epsilon=0.5$ (dotted lines). On the other hand, for $\epsilon>1$ the higher-frequency branch may occur as an optical surface SW, as is shown for $\epsilon=1.5$ (dashed lines). Figure 9 shows the results for a film with $N=9$, taking other parameters as before. One can notice that the surface SW modes in this case behave in a way that clearly contrasts with the results for even N in Fig. 8. For example, for $\epsilon=1$ (solid lines) the two surface modes are approximately degenerate for large wave vectors, but are clearly split for small wave vectors. A similar behavior occurs for $\epsilon=0.5$ (dotted lines) and $\epsilon=1.5$ (dashed lines). However, for the parameters used, there are no optical surface SW branches.

V. CONCLUSIONS

In summary we have investigated the influence of surface orientation in the spectra of spin waves in antiferromagnetic films. This represented a generalization of earlier work on antiferromagnets to incorporate the new effects arising due to finite film thickness and surface orientation. The physical importance of each was demonstated by the analytic results and numerical examples.

The calculations were performed by a method that extends the equation-of-motion formalism involving tridiagonal matrices to apply to more complicated exchange-coupled systems. Specifically, we obtained results for the exchange-dominated surface SW spectrum in films corresponding to sc antiferromagnets with surfaces on the (001), (011), and (111)

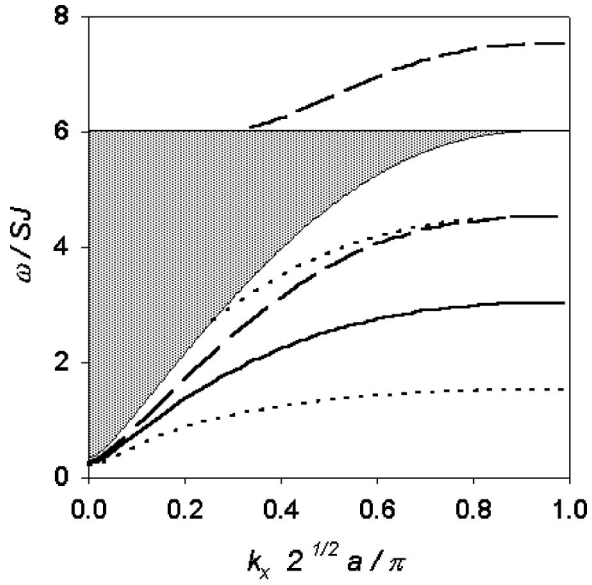

FIG. 8. Surface SW dispersion relations for a sc antiferromagnetic film with (111) surfaces and an even number of layers ($N=8$), taking $\omega_A=10^{-2}$, $\sigma=1$ and $\epsilon=0.5$ (dotted), $\epsilon=1.0$ (solid), and $\epsilon=1.5$ (dashed). The region containing the bulk modes is shaded.

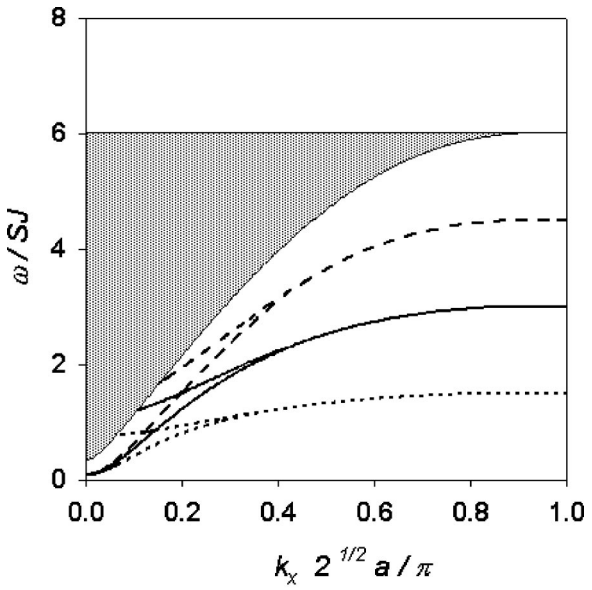

FIG. 9. Surface SW dispersion relations for sc antiferromagnetic films with (111) surfaces and an odd number of layers ($N=9$), taking $\omega_A=10^{-2}$, $\sigma=1$ and $\epsilon=0.5$ (dotted), $\epsilon=1.0$ (solid), and $\epsilon=1.5$ (dashed). The region containing the bulk modes is shaded.

crystallographic planes. For the (001) and (011) orientations, the equations of motion were simplified by using symmetric and antisymmetric combinations of the spin amplitude operators. In addition, the resulting pentadiagonal matrices were decomposed into products of tridiagonal matrices, and this allowed us to find analytical expressions for the dispersion relations. In the (111) case a different approach was employed in which the matrix equations of motion were written in a tridiagonal form by a suitable labeling of the film layers. We obtained results that show a strong dependence of the surface SW modes on the direction of propagation in the (011) orientation, as well as the effect of the inequivalence of the sublattices in the (111) film case, which is shown to introduce significant modifications on the propagation properties of the surface modes. The formalism presented here is valid for any number of layers and the semi-infinite limit can be easily obtained by making $N\rightarrow\infty$, in contrast with previous calculations,[1] where a semi-infinite medium was assumed.

This formalism can be applied to antiferromagnets such as NiO ($T_N\approx 523$ K) or the perovskite-structure $KNiF_3$ ($T_N\approx 245$ K). In both of these materials the magnetic (Ni) ions lie on a simple cubic lattice, and the exchange interactions are very strong making the use of a Heisenberg-type Hamiltonian appropriate. Since the splitting of the acoustic SW surface branches is most apparent for small wave vectors, these surface effects in films can in principle be studied experimentally by light scattering techniques. Bulk samples of the above two materials have already been studied extensively by Raman and Brillouin scattering.[9,10] A generalization of the present theoretical work could involve the inclusion of further exchange interactions (e.g., between second nearest neighbors) and application to antiferromagnetic systems with different layer coupling schemes, by analogy with our recent work for ferromagnetic Ni films with (111) surfaces.[11]

ACKNOWLEDGMENTS

This research was partially financed by the agencies CAPES of Brazil and NSERC of Canada.

APPENDIX

For the (001) case, the matrix **R** has only six nonzero elements, namely,

$$R_{1,1}=\lambda_+\lambda_- -(\lambda_+ +\lambda_-)(\omega_A+6)+2(1-\epsilon)\gamma_{\mathbf{k}}^2,$$

$$R_{1,2}=-\lambda_-, \quad R_{2,1}=\lambda_+,$$

$$R_{N-1,N}=\lambda'_+, \quad R_{N,N-1}=-\lambda'_-,$$

$$R_{N,N}=\lambda'_+\lambda'_{-2}-(\lambda'_+ +\lambda'_-)(\omega_A+6)+2(1-\epsilon')\gamma_{\mathbf{k}}^2, \tag{A1}$$

where $\lambda_\pm=1+(1-\epsilon)(4\pm\gamma_{\mathbf{k}})+(1-\sigma)\omega_A$ and $\lambda'_\pm=1+(1-\epsilon')(4\pm\gamma_{\mathbf{k}})+(1-\sigma')\omega_A$, with $\sigma=H_{AS}/H_A$ and $\sigma'=H'_{AS}/H_A$. Also **C** is a 4×4 matrix with elements defined by

$$C_{11}=R_{1,1}B_{1,1}+R_{1,2}B_{2,1}-1, \quad C_{12}=R_{1,1}B_{1,2}+R_{1,2}B_{2,2},$$

$$C_{13}=R_{1,1}B_{2,N}+R_{1,2}B_{2,N-1}, \quad C_{14}=R_{1,1}B_{1,N}+R_{1,2}B_{2,N},$$

$$C_{21}=R_{2,1}B_{1,1}, \quad C_{22}=R_{2,1}B_{1,2}-1,$$

$$C_{23}=R_{2,1}B_{2,N}, \quad C_{24}=R_{2,1}B_{1,N},$$

$$C_{31}=R_{N-1,N}B_{1,N}, \quad C_{32}=R_{N-1,N}B_{2,N},$$

$$C_{33}=R_{N-1,N}B_{1,2}-1, \quad C_{34}=R_{N-1,N}B_{1,1},$$

$$C_{41}=R_{N,N}B_{1,N}+R_{N,N-1}B_{2,N},$$

$$C_{42}=R_{N,N}B_{2,N}+R_{N,N-1}B_{2,N-1},$$

$$C_{43}=R_{N,N}B_{1,2}+R_{N,N-1}B_{2,2},$$

$$C_{44}=R_{N,N}B_{1,1}+R_{N,N-1}B_{1,2}-1. \tag{A2}$$

For the (011) case we have the redefinitions

$$R_{1,1}=(\omega_A+6)(\theta_+ +\theta_-)+\theta_+\theta_- +(\theta_+ -\theta_-)\gamma_{\mathbf{k}}^{(x)},$$

$$R_{1,2}=\theta_+\gamma_{\mathbf{k}}^{(y)}, \quad R_{2,1}=-\theta_-\gamma_{\mathbf{k}}^{(y)},$$

$$R_{N-1,N}=-\theta'_-\gamma_{\mathbf{k}}^{(y)}, \quad R_{N,N-1}=\theta'_+\gamma_{\mathbf{k}}^{(y)},$$

$$R_{N,N}=(\omega_A+6)(\theta'_+ +\theta'_-)+\theta'_+\theta'_- +(\theta'_+ -\theta'_-)\gamma_{\mathbf{k}}^{(x)}, \tag{A3}$$

where $\theta_\pm=2\epsilon-4+(1-\sigma)\omega_A\pm(1-\epsilon)\gamma_{\mathbf{k}}^{(x)}$ and $\theta'_\pm=2\epsilon'-4+(1-\sigma')\omega_A\pm(1-\epsilon')\gamma_{\mathbf{k}}^{(x)}$. For the (111) orientation, the nonzero elements of $\mathbf{R}^{(u)}$ are

$$R_{1,1}^{(u)}=g\omega_2-h\omega_1-gh+(\epsilon-1)^2\xi_{\mathbf{k}}^*\xi_{\mathbf{k}}-(3-2\epsilon)\xi_{\mathbf{k}}^*\xi_{\mathbf{k}},$$

$$R_{1,2}^{(u)}=(\epsilon-1)\xi_{\mathbf{k}}^2, \quad R_{2,1}^{(u)}=\left[\frac{(\epsilon-1)\omega_2+h}{\omega_2-h}\right](\xi_{\mathbf{k}}^*)^2,$$

$$R_{2,2}^{(u)}=\left(\frac{h}{\omega_2-h}\right)\xi_{\mathbf{k}}^*\xi_{\mathbf{k}}, \quad R_{M,M-1}^{(u)}=-\frac{g'}{\omega_2}(\xi_{\mathbf{k}}^*)^2,$$

$$R_{M,M}^{(u)}=-g'\omega_1+h'\omega_2-g'h'+(\epsilon'-1)^2\xi_{\mathbf{k}}^*\xi_{\mathbf{k}}-\left[\frac{g'}{\omega_2}-2(\epsilon'-1)\right]\xi_{\mathbf{k}}^*\xi_{\mathbf{k}}, \tag{A4}$$

and the elements of $\mathbf{C}^{(u)}$ are

$$C_{11}^{(u)}=R_{1,1}^{(u)}B_{1,1}+R_{1,2}^{(u)}B_{2,1}-1,$$

$$C_{12}^{(u)}=R_{1,1}^{(u)}B_{1,2}+R_{1,2}^{(u)}B_{2,2},$$

$$C_{13}^{(u)}=R_{1,1}^{(u)}B_{1,M}+R_{1,2}^{(u)}B_{2,M},$$

$$C_{21}^{(u)}=R_{2,1}^{(u)}B_{1,1}+R_{2,2}^{(u)}B_{2,1},$$

$$C_{22}^{(u)}=R_{2,1}^{(u)}B_{1,2}+R_{2,2}^{(u)}B_{2,2}-1,$$

$$C_{23}^{(u)}=R_{2,1}^{(u)}B_{1,M}+R_{2,2}^{(u)}B_{2,M},$$

$$C_{31}^{(u)}=R_{M,M}^{(u)}B_{M,1}+R_{M,M-1}^{(u)}B_{M-1,1},$$

$$C_{32}^{(u)}=R_{M,M}^{(u)}B_{M,2}+R_{M,M-1}^{(u)}B_{M-1,2},$$

$$C_{33}^{(u)}=R_{M,M}^{(u)}B_{M,M}+R_{M,M-1}^{(u)}B_{M,M-1}-1. \tag{A5}$$

$\mathbf{R}^{(d)}$ and $\mathbf{C}^{(d)}$ are given by similar expressions. The formalism for a (111) film with an odd number of layers is similar to the even case. For example, in the odd case the elements of the $\mathbf{R}^{(u)}$ matrices are obtained by making the replacements $h'\rightarrow 0$ and $g'\rightarrow f'$, where

$$f'=3-3\epsilon'+(1-\sigma')\omega_A-\frac{(\epsilon')^2\xi_{\mathbf{k}}\xi_{\mathbf{k}}^*}{E-(3\,\epsilon'+\omega_S')} \tag{A6}$$

and substituting $R_{M,M}^{(u)}=-f'\omega_1-(f'/\omega_2)\xi_{\mathbf{k}}^*\xi_{\mathbf{k}}$.

[1] F. Keffer, *Handbuch der Physik* (Springer-Verlag, Berlin, 1966).
[2] T. Wolfram and R.E. Dewames, Phys. Solid State **2**, 233 (1972).
[3] *Linear and Nonlinear Spin Waves in Magnetic Films and Superlattices*, edited by M. G. Cottam (World Scientific, Singapore, 1994).
[4] M.G. Cottam and D. Kontos, J. Phys. C **13**, 2945 (1980).
[5] S. Gopalan and M.G. Cottam, Phys. Rev. B **42**, 624 (1990); **42**, 10 311 (1990).
[6] N.N. Chen, M.G. Cottam, and A.F. Khater, Phys. Rev. B **51**, 1003 (1995).
[7] L.J. Jiang and M.G. Cottam, J. Appl. Phys. **85**, 5495 (1999).
[8] D.L. Mills, in *Ultrathin Magnetic Structures I*, edited by J.A.C. Bland and B. Heinrich (Springer, Berlin, 1994), p. 91.
[9] See, e.g., M.G. Cottam and D.J. Lockwood, *Light Scattering in Magnetic Solids* (Wiley, New York, 1986).
[10] M. Grimsditch, L.E. McNeil, and D.J. Lockwood, Phys. Rev. B **58**, 14 462 (1998).
[11] J. Milton Pereira, Jr. and M.G. Cottam, J. Appl. Phys. **87**, 5941 (2000).